JCTC Journal of Chemical Theory and Computation

Article

pubs.acs.org/JCTC

Understanding the Origin of the VCD Signals on the Basis of a Nonredundant Coordinate Definition

Belén Nieto-Ortega,[†] Juan Casado,[†] Juan T. López Navarrete,[†] Francisco J. Ramírez,*[,†] Matteo Tommasini,[‡] Giovanna Longhi,[§] Giuseppe Mazzeo,[§] and Sergio Abbate[§]

[†]Departamento de Química Física, Universidad de Málaga, 29071-Málaga, Spain

[‡]Dipartimento di Chimica, Materiali e Ingegneria Chimica, Politecnico di Milano, 20133 Milano, Italy

[§]Dipartimento di Medicina Molecolare e Traslazionale, Università di Brescia, 25123 Brescia, Italy

Supporting Information

ABSTRACT: The relationships between the chiroptical activity and the vibrational normal modes of epichlorohydrin have been investigated on the basis of a nonredundant internal coordinate definition not reported until now. These coordinates were verified by comparing, for the lower energy conformers, the diagonal quadratic force constants and were found to display similar values among conformers and to be consistent with the molecular structure of epichlorohydrin and its vibrational circular dichroism (VCD) spectrum. Boltzmann population factors were used to calculate the weighted sum of the individual VCD and IR spectra of the three lower energy conformers, which accurately fitted the experimental spectra of (*R*)-epichlorohydrin. The electric and magnetic transition dipole moments of the 24 vibrational normal modes were calculated for the most stable conformers. The combined analysis of these vectors and the normal mode description, given in terms of the potential energy distribution, allowed us to investigate the role of the functional groups (methylene, chlorine) and the type of internal coordinates (stretching, bending, etc.) in the chiroptical activity of the vibrations.

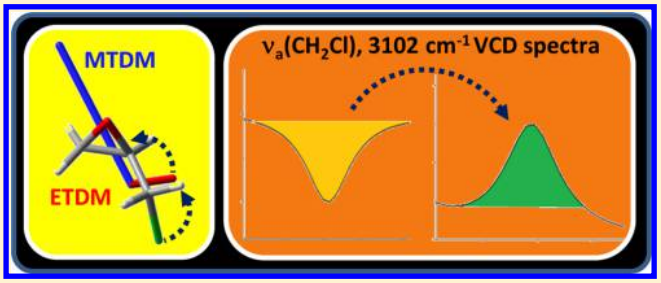

1. INTRODUCTION

The investigation of the vibrational dynamics and spectroscopic response of organic molecules by methods dealing with internal coordinates, a still active area of research, shows the interest in associating spectroscopically measurable quantities with molecular properties which can be defined at the level of the chemical group. Nowadays Quantum Chemistry allows to model accurately vibrational spectra by means of Cartesian coordinates which are undoubtedly the most efficient computational choice. However, the interpretation of vibrational spectra from the point of view of local molecular properties related with chemical groups or bonds still requires a transformation to a suitable set of internal coordinates. Due to the very mathematical nature of the problem, for a given molecule several choices of internal coordinates may be possible and may highlight different aspects of the vibrational dynamics.

Circular dichroism, namely the differential absorption of right and left circularly polarized light, is a property exhibited by any molecule not superimposable to its mirror image. Since 1884 these molecules have been called chiral,[1] and their mirror images, or enantiomers, are optical isomers. The classical definition of chirality is associated with the existence of an asymmetric carbon atom,[2] the first known source of optical activity in molecules. Later, chiral axes and chiral planes extended this concept to compounds without asymmetric carbons, even without any carbon atom. Thus, the modern concept of chirality is based on the overall molecular symmetry: an object is chiral if it does not possess any improper axis as symmetry element. In consequence, the molecules belonging to the C_1, C_n, or D_n point groups are chiral, all others being achiral.

Several forms of chiroptical spectroscopies are available, encompassing rotation of the light polarization plane or differential scattering, absorption and fluorescence phenomena. Circular dichroism belongs to absorption phenomena and consists of the difference in absorption of left and right circularly polarized light from the different optical isomers of a chiral molecule. The technique has been developed in two main branches, which cover electronic (ECD) and vibrational (VCD) transitions between molecular states.[3−9] From a structural point of view, in condensed phase, a vibrational spectrum gives us greater information than an electronic spectrum because it contains a large number of measurable bands, which can be accurately assigned to motions of specific atoms within the molecules. This concept, widely known when comparing infrared spectroscopy with electronic absorption, is also applicable to VCD and ECD. Furthermore, ECD is exhibited only by molecules having a chromophore, while virtually all chiral molecules give VCD signals. However, the greater power of VCD over ECD may not be immediately

Received: December 17, 2014
Published: May 6, 2015

DOI: 10.1021/acs.jctc.5b00106
J. Chem. Theory Comput. 2015, 11, 2633−2641

exploited. Reliable interpretation of any infrared spectrum is more troublesome than the electronic spectrum of the same system because the former is better understood on the basis of a thorough definition of vibrational coordinates. From the experimental viewpoint, VCD requires longer acquisition times and higher concentrations than ECD because it is a hundred times weaker effect (typical g values of $10^{-3}-10^{-4}$ for VCD and $10^{-1}-10^{-2}$ for ECD; g is the dissymmetry factor, defined as the ratio between the intensities of circular dichroism and absorption).

The previous paragraph suggests that, once we obtain a complete set of vibrational coordinates, the interpretation of a vibrational spectrum may become a straightforward task. In fact, this is rather true for classical infrared spectroscopy, where reliable correlations exist in terms of peak position and intensities. However, the relationships between the sign and intensity of a specific VCD band and its description in terms of vibrational coordinates has been scarcely studied,[10] in spite of the fact that the VCD spectrum of a medium size molecule may be easily calculated by quantum chemistry methods. This is the topic addressed in this work.

To meet this challenge we chose epichlorohydrin (Figure 1), a small molecule widely used as intermediate in the synthesis of

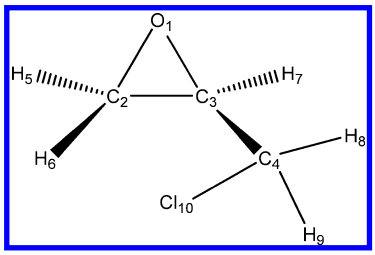

Figure 1. Chemical structure of (*R*)-epichlorohydrin and atom numbering used throughout.

glycidyl ether based epoxy resins.[11] This molecule possesses an asymmetric carbon which gives rise to two enantiomers, (*R*) and (*S*), which also present conformational isomerism due to the internal rotation of the chloromethyl side chain. In a previous work,[12] the absolute configuration of epichlorohydrin was determined using quantum chemistry and VCD spectroscopy, while vibrational spectroscopy was interpreted on the basis of a basic valence internal coordinate definition (bond stretchings, interbond angle bendings, torsions, out-of-plane bendings), useful for a pictorial, easy-to-understand analysis but not supported by a consistent force field.

The aim of the present work is to find relationships between the VCD features and the nature of the vibrational transitions of epichlorohydrin. To address this issue it is mandatory to come up with a definition of internal coordinates that can be supported by reliable values of the quadratic force constants. We also need to carry out a conformational analysis, based on quantum chemistry calculations, to determine the most stable conformations of the molecule. VCD spectra and force constants will be evaluated for each conformer, and the experimental VCD spectrum will be compared with the weighted sum of the individual spectra of the conformers. The electric and magnetic transition dipole moments, which originate the chiroptical activity, will be calculated for the vibrations of each conformer. The goal of this study will be achieved by relating the transition dipole moment values to the vibrational potential energy provided by the internal coordinates previously defined.

2. COMPUTATIONAL METHODS

The Gaussian'09 suite of programs[14] was used to carry out the DFT quantum chemical calculations presented here. The Becke's three parameter (B3)[13] gradient-corrected exchange functional was used, and the nonlocal correlation was provided by the Lee−Yang−Parr (LYP) expressions.[15,16] Ground-state structures were calculated using the split-valence 6-311G-(2p,2d) basis set.[17,18] Solvent effect was incorporated using the Polarizable Continuum Model (PCM) to simulate a CCl_4 environment.[19,20]

Harmonic force constants were analytically computed on the ground-state minimum-energy structures, from which vibrational normal mode wavenumbers, intensities, and the corresponding vibrational atomic displacements, within the space of 3*N* Cartesian coordinates, were evaluated. This force field was then transformed to a space of 3*N*−6 locally symmetrized vibrational coordinates, S_k, $k = 1\cdots 3N-6$, orthogonal to the redundancy conditions and defined as linear combinations of stretching, bending, or torsion internal vibrations, *R*.[21−24] Such combinations also have the advantage of removing local and cyclic redundancies, which are often present in organic molecules, as in the case of epichlorohydrin.

In this paper we follow the method proposed by Pulay et al.[25,26] to remove systematically all redundancies occurring in our systems. In matrix notation, the linear transformations between coordinates are

$$R = Bx; \qquad S = UR \tag{1}$$

Then the potential energy in Cartesian coordinates

$$2V = x^t F_x x \tag{2}$$

can be re-expressed in terms of the *S* coordinates as

$$2V = S^t U^{-1t} B^{-1t} F_x B^{-1} U^{-1} S \tag{3}$$

where the *B* matrix contains the linear combinations to transform the Cartesian coordinates to the internal coordinates.[27] For the solution of the vibrational problem for finite molecules we use the eigenvalue equation proposed by Wilson et al.[21]

$$\boldsymbol{G_S F_S L_S} = \boldsymbol{L_S \Lambda} \tag{4}$$

where $\boldsymbol{G_S}$ is the inverse of the kinetic energy matrix in the new internal coordinates and contains information about the atoms which constitute the molecule and their equilibrium positions, $\boldsymbol{F_S}$ is the matrix of the Pulay force constants, $\boldsymbol{L_S}$ is the matrix of the vibrational amplitudes, and $\boldsymbol{\Lambda}$ is the diagonal eigenvalue matrix.[21] The normal mode wavenumbers, ν_i, in cm^{-1}, can be computed from the eigenvalues of the *GF* matrix, λ_i, in s^{-2}, called frequency parameters through the relation

$$\nu_i = \left(\frac{\lambda_i}{4\pi^2 c^2}\right)^{1/2} \tag{5}$$

The theoretical spectra were obtained from the DFT intensities in combination with the calculated vibrational wavenumbers and were uniformly scaled with a single scaling factor (0.98) while keeping the calculated intensities unchanged, in order to better compare with experimental spectra. Every band was represented by a Gaussian function of 20 cm^{-1} half-height width.

DOI: 10.1021/acs.jctc.5b00106
J. Chem. Theory Comput. 2015, 11, 2633−2641

3. EXPERIMENTAL SETTINGS

The samples of epichlorohydrins (*R* and *S*) were obtained from Aldrich Chemical Co. at a stated purity of 99%. Infrared spectra were recorded at room temperature using a Bruker Vertex 70 Fourier transform (FT) spectrometer purged with dry N_2 gas. Typically, 64 scans at a resolution higher than 4 cm^{-1} were accumulated to optimize the signal-to-noise ratio. Individual scans were examined by the recording routine before averaging, being automatically discarded when the mean intensity deviations were greater than 10% over the full interferogram length.

VCD spectra were measured by means of a Bruker PMA50 optical bench coupled to the Vertex 70 spectrometer. In the PMA50 instrument, the infrared radiation is focused by a BaF_2 lens, passing an optical filter (3800−600 cm^{-1} range) and a ZnSe photoelastic modulator (PEM, 50 kHz frequency). The light beam is finally collected by a D313/QMTC detector with nondichroic BaF_2 windows. Previous calibration of the PEM at a fixed wavenumber is required before recording a VCD spectrum. A spectral region of 600 cm^{-1} centered on each calibration wavenumber is then available. Typically, calibrations at 1300 cm^{-1} allowed us to obtain VCD signals for the complete infrared region of interest. Every VCD spectrum was the result of averaging a minimum of 28000 scans (12 h acquisition time) at a spectral resolution of 4 cm^{-1}.

Infrared and VCD spectra were recorded on solutions in CCl_4 at a 2 M concentration. A variable path liquid cell of 0.025 mm length, with KBr windows, was used for all the measurements. Spectral treatment were carried out using the OPUS 6.5 © software.

4. RESULTS AND DISCUSSION

4.1. Conformational Analysis and Theoretical Spectra. The first goal of this work was to determine the more stable conformations of epichlorohydrin. Calculations were carried out for the (*R*)-enantiomer, for which the following steps were considered:

i) Structural optimization up to the minimal energy point was reached by allowing all geometrical parameters to vary independently.

ii) Energy scanning over 360 deg. rotation around the C3−C4 bond. The energy profile obtained is included in Figure FS1 of the Supporting Information (SI).

iii) Structural optimization of the three conformers and calculation of their infrared and VCD spectra.

Figure 2 summarizes the relative Gibbs free energies and relative population factors, at 298.15 K, calculated by supposing a thermodynamic equilibrium (see equation inserted) among the three most stable conformers, using a cutoff of 2.0 kcal/mol. The results are in agreement with the conformational isomerism reported for the (*S*)-enantiomer using CCl_4 as solvent,[12,31] which also included a minor contribution of the C_{III} conformer. The latter conformer is also named *cis* due to the relative position of the chlorine atom with respect to the epoxide ring. In the two lower energy conformers, also named the *gauche* forms, the chlorine atom is oriented farther from the ring.[28]

The theoretical infrared and VCD spectra of the three conformers are shown in Figure 3. At first glance, the differences in the three calculated infrared spectra are quite large, taking into account that the conformational isomerism is exclusively due to the rotation of the CH_2−Cl moiety. Even

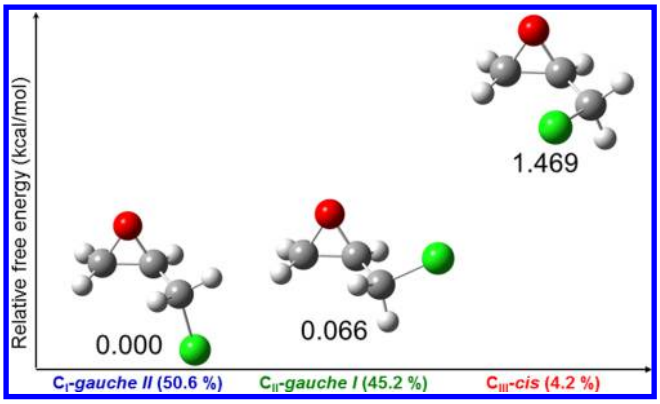

Figure 2. Conformations, relative free energies and concentrations of the three lower energy conformers of (*R*)-epichlorohydrin.

greater differences are observed in the calculated VCD spectra, where some bands display also sign inversion. In the averaged spectrum some of them may be offset, but, all the same, the bands with noticeable wavenumber shifts give rise to an overmultiple signal, which may be used as a strong evidence of the calculated absolute configuration.

4.2. Infrared and VCD Spectroscopy. Figure 4 compares the experimental infrared and VCD spectra of (*R*)-epichlorohydrin, in the 1600 and 800 cm^{-1} region, with those obtained by summing the calculated spectra of the three conformers (Figure 3) conveniently weighted by their relative concentrations. They were compared with the spectra of the (*S*)-enantiomer (Figure FS2 of the SI), showing mirror-like VCD responses for two almost identical infrared spectra.

As aforementioned, an overmultiple signal is found between 1550 and 1350 cm^{-1}, where only three fundamentals are expected for the bending vibrations of two methylenes and a methyne groups (see the individual spectra of Figure 3). Instead, no less than four bands are clearly observed in this infrared region. Similarly, between 1300 and 1200 cm^{-1} we should assign two fundamentals, while a broad intense IR absorption band composed by more than three components is observed. These facts indicate the presence of at least two conformers with appreciable concentrations, as a consequence of the prediction of the absolute configuration. This same observation was previously made by Polavarapu et al.[12] On the other hand, the match between the experimental and the averaged infrared and VCD spectra is quite satisfactory, which gives us a solid support to investigate the origin of the vibrational chiroptical signal in terms of relationships between the VCD features and the normal mode descriptions. Table 1 summarizes the experimental and the calculated wavenumbers in this region.

4.3. Normal Mode Analysis. The first step in the way of finding useful correlations between the chiroptical VCD signal and the nature of the underlying normal mode vibration is to build a reliable set of nonredundant internal coordinates able to give a correct image of the vibrating molecule. These coordinates must provide us a suitable description of all the fundamentals and, no less important, a set of force constants consistent with the molecular structure which should take comparable values among the different conformers. For epichlorohydrin, the complete list of coordinates includes 10 stretching coordinates, one for each bond, 8 bending coordinates for the two methylene group, 2 bending coordinates for the methyne group, 3 bending coordinates of

DOI: 10.1021/acs.jctc.5b00106
J. Chem. Theory Comput. 2015, 11, 2633−2641

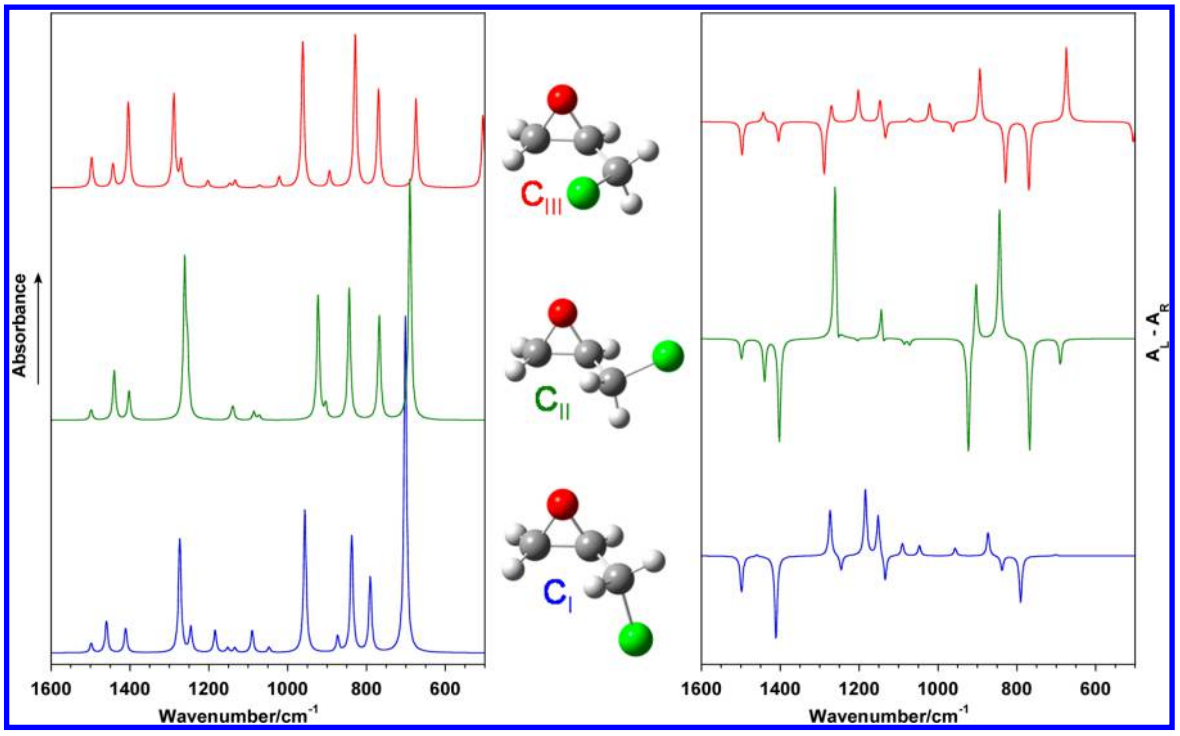

Figure 3. Theoretical infrared and VCD spectra of the three lower energy conformers of (*R*)-epichlorohydrin.

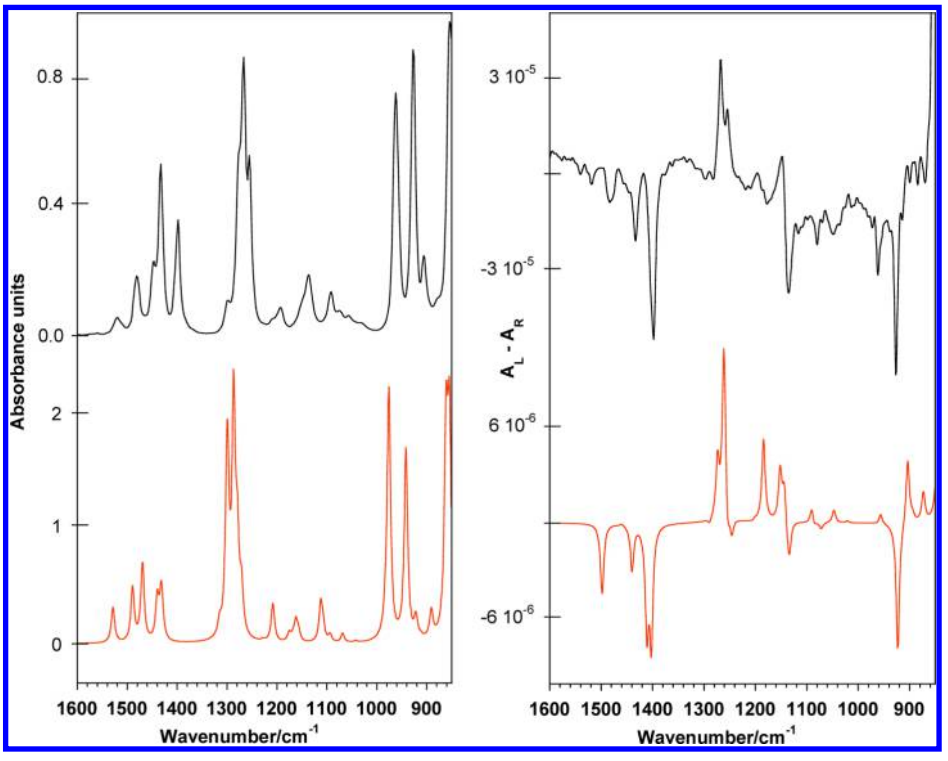

Figure 4. Experimental (black) and theoretical (red) infrared and VCD spectra of (*R*)-epichlorohydrin.

the CH_2Cl group, and 1 torsion coordinate of the C−C bond. The precise definition of these 24 normalized coordinates, together with the three redundant coordinates which are orthogonal with any of them, is summarized in Table 2. This means that any scalar product between coefficients of redundant and nonredundant coordinates is always zero, as for instance

$$S_{12}{}^{*}\Pi_1 = {}^{1}/_{2}[0, 0, 1, -1, 1, -1]^{*}[1, 1, 1, 1, 1, 1]$$
$$= {}^{1}/_{2}(1 - 1 + 1 - 1) = 0$$

In particular, among the coordinates of the three-membered ring of epichlorohydrin, only CC or CO stretches were admitted, and neither CCO nor COC bending was included; this is different from what was done by Pulay et al.,[25,26] e.g. we made sure that all coordinates were orthogonal to redun-

DOI: 10.1021/acs.jctc.5b00106
J. Chem. Theory Comput. 2015, 11, 2633−2641

Table 1. Calculated and Experimental Vibrational Wavenumbers (in cm^{-1}) for (*R*)-Epichlorohydrin

experimental[a]	C_I	C_{II}	C_{III}
1480m	1498	1498	1496
1447m/1433s	1459	1439	1442
1398m	1410	1402	1403
1275sh/1266vs/1297w	1273	1261	1287
1255s	1245	1253	1270
1193*w*/1205sh	1183	1203	1201
1143sh	1151	1143	1146
1136m	1133	1138	1132
1092*m*/1076w	1089	1085	1071
1056*w*/1032sh	1046	1071	1021
961vs/926vs	956	922	961
876sh/906m	873	903	893
854vs	837	843	828

[a]Relative intensities are s = strong, m = medium, w = weak, sh = shoulder, v = very.

dancies. This has the consequence that no arbitrary constant has to be added to the values of the diagonal force constants, which are included in Table TS1 of the SI. Two observations can be made: (i) for each internal coordinate, the values of the diagonal force constants for the three conformers are within narrow ranges; the higher deviations are lower than 0.2 (in mdyne/Å for stretches or in mdyneÅ/rad^2 for bending coordinates), with the exception of ϕ(C−C) which goes from 0.85 mdyne·Å/rad^2 in C_I to 1.12 mdyne·Å/rad^2 in C_{III}; (ii) in all the conformers the values are consistent with the usual values for stretching, bending, and torsion coordinates in similar systems, e.g. all the force constants have a coherent physical meaning, which is a solid support to this study. This also ensures to reach a reliable description of the 24 normal modes of each conformer in terms of the vibrational potential energy distribution based on the defined internal coordinates. This is shown in Tables 3, 4, and 5, which allows one to provide an assignment to each normal mode, by naming it on the basis of the highest value of the Potential Energy Distribution (PED). This name then is unambiguous, except for the central region of the spectra, namely between 1100 and 900 cm^{-1}, where extensive mixing appears, and very similar PED values are found for three internal coordinates, making it impossible to make a clear-cut assignment (*vide infra*).

4.4. Transition Dipole Moments. The VCD intensity of a transition between two vibrational states, φ_i and φ_j, is given by the Rosenfeld equation[29]

$$\int \Delta\varepsilon d\nu \alpha R_{ij} \approx \mathrm{Im}(\vec{\mu}_{ij}\cdot\vec{m}_{ji}) = |\vec{\mu}_{ij}|\cdot|\vec{m}_{ji}|\cdot\cos\theta$$

where R_{ij} is the rotatory strength (which is related with the intensity of the chiroptical signal), $|\vec{\mu}_{ij}|$ is the magnitude of the electric transition dipole moment $\vec{\mu}_{ij}$ (ETDM), $|\vec{m}_{ji}|$ is the magnitude of the magnetic transition dipole moment $\vec{m}_{ji}$ (MTDM), and θ is the angle formed by these two vectors, which ultimately determines the sign of the band. When the intensity of a VCD band is largely due to a high value of the module of either one of the two transition dipole moments, the vibration is named either electric dipole allowed (*eda*) or magnetic dipole allowed (*mda*) respectively. Since the IR activity depends only on the magnitude of the ETDM vector, the *eda* vibrations are always associated with intense infrared bands, while the *mda* vibrations exhibit very low infrared

Table 2. Internal Coordinates Defined for (*R*)-Epichlorohydrin

no.	coordinate[a]	symbol	description
1	$2^{-1/2}$ ($r_{2\,5}$ + $r_{2\,6}$)	$\nu_s(CH_2)$	CH_2 sym. stretching
2	$2^{-1/2}$ ($r_{2\,5}$ − $r_{2\,6}$)	$\nu_a(CH_2)$	CH_2 antisym. stretching
3	$r_{3\,7}$	ν(CH)	C−H stretching
4	$2^{-1/2}$ ($r_{4\,8}$ + $r_{4\,9}$)	$\nu_s(CH_2Cl)$	CH_2Cl sym. stretching
5	$2^{-1/2}$ ($r_{4\,8}$ − $r_{4\,9}$)	$\nu_a(CH_2Cl)$	CH_2Cl antisym. stretching
6	$r_{4\,10}$	ν (CCl)	C−Cl stretching
7	$r_{3\,4}$	ν (CC)	C−C stretching
8	$r_{2\,3}$	ν(ring)	ring stretching
9	$r_{1\,2}$	ν(ring)	ring stretching
10	$r_{1\,3}$	ν(ring)	ring stretching
11	$20^{-1/2}$ ($4\beta_{5\,2\,6}$ − $\beta_{1\,2\,6}$ − $\beta_{3\,2\,5}$ − $\beta_{1\,2\,5}$ − $\beta_{3\,2\,6}$)	$\delta(CH_2)$	CH_2 scissoring
12	1/2 ($\beta_{1\,2\,6}$ − $\beta_{3\,2\,5}$ + $\beta_{1\,2\,5}$ − $\beta_{3\,2\,6}$)	$\omega(CH_2)$	CH_2 wagging
13	1/2 ($\beta_{1\,2\,6}$ + $\beta_{3\,2\,5}$ − $\beta_{1\,2\,5}$ − $\beta_{3\,2\,6}$)	t(CH_2)	CH_2 twisting
14	1/2 ($\beta_{1\,2\,6}$ − $\beta_{3\,2\,5}$ − $\beta_{1\,2\,5}$ + $\beta_{3\,2\,6}$)	r(CH_2)	CH_2 rocking
15	$20^{-1/2}$ ($4\beta_{8\,4\,9}$ − $\beta_{3\,4\,8}$ − $\beta_{9\,4\,10}$ − $\beta_{3\,4\,9}$ − $\beta_{8\,4\,10}$)	$\delta(CH_2Cl)$	CH_2Cl scissoring
16	1/2 ($\beta_{3\,4\,8}$ − $\beta_{9\,4\,10}$ + $\beta_{3\,4\,9}$ − $\beta_{8\,4\,10}$)	$\omega(CH_2Cl)$	CH_2Cl wagging
17	1/2 ($\beta_{3\,4\,8}$ + $\beta_{9\,4\,10}$ − $\beta_{3\,4\,9}$ − $\beta_{8\,4\,10}$)	t(CH_2Cl)	CH_2Cl twisting
18	1/2 ($\beta_{3\,4\,8}$ − $\beta_{9\,4\,10}$ − $\beta_{3\,4\,9}$ + $\beta_{8\,4\,10}$)	r(CH_2Cl)	CH_2Cl rocking
19	$2^{-1/2}$ ($\beta_{1\,3\,7}$ − $\beta_{2\,3\,7}$)	ϕ(CH)	CH out-plane bending
20	$2^{-1/2}$ ($\beta_{1\,3\,7}$ − $\beta_{4\,3\,7}$)	δ(CH)	CH in-plane bending
21	$2^{-1/2}$ ($\beta_{1\,3\,4}$ − $\beta_{2\,3\,4}$)	ω(CC)	C−C wagging
22	$6^{-1/2}$ ($2\beta_{4\,3\,7}$ − $\beta_{1\,3\,4}$ − $\beta_{2\,3\,4}$)	δ(CC)	C−C in-plane bending
23	$30^{-1/2}$ ($5\beta_{3\,4\,10}$ − $\beta_{8\,4\,9}$ − $\beta_{3\,4\,8}$ − $\beta_{9\,4\,10}$ − $\beta_{3\,4\,9}$ − $\beta_{8\,4\,10}$)	ϕ(CC)	C−C out-plane bending
24	$\tau_{3\,4}$	$\tau(CH_2Cl)$	CH_2Cl torsion
25	$\beta_{5\,2\,6}$ + $\beta_{1\,2\,3}$ + $\beta_{1\,2\,6}$ + $\beta_{3\,2\,5}$ + $\beta_{1\,2\,5}$ + $\beta_{3\,2\,6}$	Π_1	*redundant*[b]
26	$\beta_{5\,2\,6}$ + $\beta_{1\,2\,3}$ + $\beta_{1\,2\,6}$ + $\beta_{3\,2\,5}$ + $\beta_{1\,2\,5}$ + $\beta_{3\,2\,6}$	Π_2	*redundant*[b]
27	$\beta_{5\,2\,6}$ + $\beta_{1\,2\,3}$ + $\beta_{1\,2\,6}$ + $\beta_{3\,2\,5}$ + $\beta_{1\,2\,5}$ + $\beta_{3\,2\,6}$	Π_3	*redundant*[b]

[a]See Figure 1 for atomic numbering; r_{ij} is the stretching vibrations of the bond between atoms *i* and *j*; β_{ijk} is the vibration of the angle between atoms *i*, *j*, and *k*; τ_{ij} is the torsion vibration with respect to the bond between atoms *i* and *j*. [b]The scalar product of any of the coordinates 1−24 by any of the coordinates 25−27 is zero (orthogonal).

intensities. Thus, in order to know the origin of the chiroptical signal it is necessary to calculate the EDTM and the MDTM vectors and the angle between them.[30] All these data are included in Tables 3−5 for the three conformers of (*R*)-epichlorohydrin, together with the description of each normal mode in terms of the PED. A graphical representation of some selected examples, useful for discussion below, is shown in Figure 5.

Let us analyze the different calculated IR and VCD bands, with particular attention to a selected set, the EDTM and MDTM of which are reported in Figure 5. In the 3000−3200 cm^{-1} region, the antisymmetric stretching vibrations of the two methylene groups, $\nu_a(CH_2)$ and $\nu_a(CH_2Cl)$, have larger MDTM magnitudes than the symmetric ones, while their EDTM values are similar. They are therefore strong *mda* modes whose transition dipole moments, in the three conformers, are

DOI: 10.1021/acs.jctc.5b00106
J. Chem. Theory Comput. 2015, 11, 2633−2641

Table 3. Associated Transition Dipole Moments and Normal Mode Description of the Calculated Wavenumbers of Conformer C_I of (*R*)-Epichlorohydrin[a]

wn (cm^{-1})	VCD int.	ETDM	MTDM	θ (deg)	PED (potential energy distribution; values >10%)
3127	1.91	5.09	12.79	88.32	98 $\nu_a(CH_2)$
3103	−6.48	2.54	9.49	105.60	94 $\nu_a(CH_2Cl)$
3068	−3.21	3.77	3.02	106.40	94 $\nu(CH)$
3041	6.39	3.55	1.88	17.50	99 $\nu_s(CH_2Cl)$
3037	2.37	5.55	8.18	87.01	99 $\nu_s(CH_2)$
1498	−6.27	2.45	3.22	142.80	89 $\delta(CH_2)$ + 13 ν(ring)
1459	0.34	4.57	2.27	88.13	94 $\delta(CH_2Cl)$
1410	−15.20	4.07	4.80	141.21	72 δ(CH) + 33 δ(CC) + 25 ν(ring) + 13 $\delta(CH_2)$
1273	9.45	9.37	4.46	76.94	47 $\omega(CH_2Cl)$ + 31 δ(CH) + 20 ν(ring)
1245	−3.15	4.42	4.60	98.93	49 $\omega(CH_2Cl)$ + 42 δ(CH) + 17 ν(ring)
1183	15.54	4.27	3.81	26.61	47 $t(CH_2Cl)$ + 16 ν(CC) + 12 $t(CH_2)$
1151	9.24	2.06	4.56	10.67	53 ϕ(CH) + 25 $r(CH_2)$ + 20 δ(CH) + 16 $\omega(CH_2)$
1133	−4.87	2.05	3.39	134.33	76 $\omega(CH_2)$
1089	2.95	4.45	4.00	80.43	29 $t(CH_2)$ + 20 $r(CH_2)$ + 12 $t(CH_2Cl)$
1046	2.54	2.23	3.71	72.11	35 ϕ(CH) + 23 $t(CH_2Cl)$ + 19 $r(CH_2)$ + 12 ν(CC) + 10 $r(CH_2Cl)$ + 10 δ(CC)
956	2.11	12.06	3.65	87.26	34 ν(ring) + 20 ν(CC) + 16 $t(CH_2)$ + 16 $r(CH_2Cl)$
873	6.94	4.20	6.19	74.53	47 $r(CH_2Cl)$ + 34 $t(CH_2)$ + 14 $r(CH_2)$ + 11 ϕ(CH)
837	−4.51	11.68	4.42	95.02	89 ν(ring) + 10 ν(CC)
790	−15.47	9.66	7.70	102.01	81 ν(ring)
700	0.60	21.61	4.64	89.66	89 ν(CCl) + 12 ϕ(CC)
398	0.72	1.53	2.05	76.66	49 ω(CC) + 23 δ(CC) + 10 ϕ(CC) + 10 ν(CCl)
360	7.95	7.06	1.55	43.51	71 δ(CC) + 15 ν(CCl)
203	13.20	16.32	2.15	67.93	74 ϕ(CC) + 37 ω(CC)
88	−22.18	19.34	1.36	147.38	102 $\tau(CH_2Cl)$

[a]The symbols correspond to the coordinates listed in Table 5. Coordinates with similar characters were added to clarify. The VCD intensities are presented as the rotational strengths, *R*, in 10^{-44} esu^2 cm^2.

Table 4. Associated Transition Dipole Moments Description of the Calculated Wavenumbers of Conformer C_{II} of (*R*)-Epichlorohydrin[a]

wn (cm^{-1})	VCD int.	ETDM	MTDM	θ (deg)	PED (potential energy distribution; values >10%)
3122	2.27	5.24	17.08	88.65	98 $\nu_a(CH_2)$
3102	1.98	2.17	7.59	83.06	94 $\nu_a(CH_2Cl)$
3067	0.01	3.79	1.47	89.87	95 ν(CH)
3038	−7.4	5.04	1.58	157.92	94 $\nu_s(CH_2Cl)$
3034	2.8	5.02	5.36	84.04	95 $\nu_s(CH_2)$
1498	−3.44	2.59	2.50	122.24	92 $\delta(CH_2)$ + 15 ν(ring)
1439	−7.52	5.79	2.75	118.09	87 $\delta(CH_2Cl)$
1402	−19.01	4.46	4.29	172.85	89 δ(CH) + 37 δ(CC) + 21 ν(ring) + 11 $\delta(CH_2Cl)$
1261	32.63	10.89	3.48	30.87	56 $\omega(CH_2Cl)$ + 49 δ(CH)
1253	−5.69	6.51	5.15	99.79	46 ν(ring) + 41 $\omega(CH_2Cl)$ + 16 δ(CH)
1203	−0.59	0.62	3.70	105.00	58 $t(CH_2Cl)$ + 10 ν(CC)
1143	7.74	1.71	4.97	24.49	54 $\omega(CH_2)$ + 23 ϕ(CH) + 19 $r(CH_2)$
1138	−3.03	3.28	4.02	103.32	36 $\omega(CH_2)$ + 28 ϕ(CH) + 19 $r(CH_2)$
1085	−1.22	2.80	2.56	99.79	25 ν(CC) + 21 $t(CH_2Cl)$ + 20 δ(CC) + 12 $t(CH_2)$ + 12 $r(CH_2)$
1071	−1.44	2.05	2.80	104.54	34 ϕ(CH) + 25 $r(CH_2)$ + 23 $t(CH_2)$
922	−32.51	11.50	6.92	114.16	40 ν(ring) + 23 $t(CH_2)$ + 20 $r(CH_2Cl)$
903	16.91	3.82	7.06	51.16	43 ν(ring) + 40 $r(CH_2Cl)$ + 19 ν(CC)
843	39.41	12.32	6.17	58.27	44 ν(ring) + 22 $t(CH_2)$
767	−38.29	11.50	3.72	152.41	78 ν(ring)
689	−9.47	18.42	2.91	100.17	86 ν(CCl) + 16 ϕ(C−C)
427	45.49	13.21	4.74	43.41	42 δ(CC) + 31 ω(CC) + 13 $r(CH_2)$ + 10 ϕ(CC)
356	−9.61	5.46	2.55	133.47	57 δ(CC) + 18 ν(CCl)
204	−4.57	2.06	2.63	147.35	63 ϕ(CC) + 45 ω(CC)
88	−6.93	7.70	1.57	122.17	95 $\tau(CH_2Cl)$

[a]The symbols correspond to the coordinates listed in Table 5. Coordinates with similar characters were added to clarify. The VCD intensities are presented as the rotational strengths, *R*, in 10^{-44} esu^2 cm^2.

smaller in $\nu_a(CH_2Cl)$ than in $\nu_a(CH_2)$, as can be observed in Figure 5. In the case of the conformer C_{III}, where the chlorine atom is directed toward the epoxide ring, we calculated a large coupling between $\nu_s(CH_2Cl)$ and ν(CH) coordinates in the 3019 and 3032 cm^{-1} wavenumbers (Table 5), which was not obtained for conformers C_I and C_{II}. In this region, the only normal mode that preserves its chiroptical sign (+) in the three conformers is the $\nu_a(CH_2)$. The values of θ angle for this vibration are just below 90 deg, which originates weak positive VCD bands in the three conformers. The most intense chiroptical features in this region are assigned to the two $\nu_s(CH_2Cl)$ vibrations in the conformers C_I and C_{II}. The C_{III} conformer does not follow this trend, its most intense VCD band being assigned to the $\nu_s(CH_2)$. Nevertheless, previous data reported for the (*S*)-enantiomer[31] suggest the existence of anharmonic interactions in this region, e.g. Fermi resonance involving the C−H stretching vibrations, which hinders the matching between the theoretical and the experimental spectra in this region.

All three conformers show three infrared bands between 1400 and 1500 cm^{-1}, which are assigned, in a decreasing order of wavenumber, to $\delta(CH_2)$, $\delta(CH_2Cl)$, and δ(CH) bending modes. Their VCD activities are largely modulated by the angle between the two transition dipole moments, θ, since their magnitudes are similar for the three conformers (see Tables 3−5 and Figure 5). As for the C−H stretching vibrations, the signs of the VCD bands assigned to $\delta(CH_2)$ and δ(CH) are invariant for the three conformers, although in this case they are negative. On the opposite, the chiroptical signal associated with $\delta(CH_2Cl)$ is strikingly different for each conformer. The θ value for δ(CH) is smaller in the C_{III} conformer than in C_I and C_{II}, which makes its chiroptical feature appreciably weaker for the less abundant conformer. The proximity of the chlorine atom also modulates the chiroptical behavior of the two methylene wagging vibrations, with $\omega(CH_2Cl)$ contributing between 1200 and 1300 cm^{-1} and $\omega(CH_2)$ contributing between 1100 and 1200 cm^{-1}. Interestingly, the VCD sign of the methylene wagging of the CH_2Cl group discriminates the C_{III} conformer from the others, while it is invariant, once again, for the methylene group attached to the epoxide ring. Besides, in the three conformers the two $\omega(CH_2)$ are *mda*, whereas the two $\omega(CH_2Cl)$ modes are *eda*, giving rise to intense infrared absorption bands.

DOI: 10.1021/acs.jctc.5b00106
J. Chem. Theory Comput. 2015, 11, 2633−2641

Table 5. Associated Transition Dipole Moments Description of the Calculated Wavenumbers of Conformer C_{III} of (*R*)-Epichlorohydrin[a]

wn (cm^{-1})	VCD int.	ETDM	MTDM	θ (deg)	PED (potential energy distribution; values >10%)
3136	2.68	4.22	11.50	86.86	98 $\nu_a(CH_2)$
3081	3.12	1.91	10.28	80.85	100 $\nu_a(CH_2Cl)$
3044	−8.59	5.69	2.69	124.16	95 $\nu_s(CH_2)$
3032	8.58	6.85	1.40	26.64	24 ν (CH) + 74 $\nu_s(CH_2Cl)$
3019	3.41	2.56	2.54	58.24	74 ν (CH) + 26 $\nu_s(CH_2Cl)$
1496	−5.79	4.42	3.38	112.80	89 $\delta(CH_2)$ + 22 ν(ring)
1442	1.77	3.94	1.76	75.22	98 $\delta(CH_2Cl)$
1403	−3.65	7.70	2.65	100.35	79 δ(CH) + 35 δ(CC) + 26 ν(ring) + 17 $\delta(CH_2)$ + 13 ν(CC)
1287	−10.75	8.38	3.08	114.64	91 $\omega(CH_2Cl)$ + 15 ν(CC)
1270	3.78	4.45	5.54	81.17	83 δ(CH) + 28 ν(ring) + 14 δ(CC)
1201	6.9	2.35	6.00	60.70	70 t(CH_2Cl) + 13 ϕ(CH)
1146	5.15	1.76	4.18	45.67	75 $\omega(CH_2)$ + 14 ϕ(CH)
1132	−4.16	2.49	4.53	111.67	42 r(CH_2) + 28 ϕ(CH) + 20 $\omega(CH_2)$
1071	0.8	1.46	2.95	79.21	38 t(CH_2) + 24 ϕ(CH) + 14 r(CH_2) + 12 δ(CH)
1021	4.6	3.21	3.11	62.48	28 δ(CC) + 27 t(CH_2) + 20 ϕ(CH) + 18 r(CH_2) + 15 ν(CC)
961	−2.7	12.22	4.69	92.70	35 ν(ring) + 20 ν(CC) + 20 r(CH_2Cl)
893	15.6	4.17	8.80	64.84	37 ν(ring) + 35 r(CH_2Cl) + 13 ν(CC)
828	−19.21	13.44	7.25	101.40	67 ν(ring) + 18 r(CH_2Cl)
769	−23.1	11.14	2.71	140.02	45 ν(ring) + 18 ν(CCl) + 12 ν(CC) + 10 ϕ(CH)
674	28.75	11.33	3.07	34.32	52 ν(CCl) + 23 ϕ(CC) + 10 ν(CC)
503	−10.26	11.79	3.80	103.24	38 δ(CC) + 36 ν(CCl) + 16 ϕ(CC)
345	4.60	10.32	2.94	81.27	107 ω(CC)
196	1.66	3.62	1.40	70.84	50 ϕ(CC) + 45 δ(CC)
105	1.54	12.57	1.34	84.73	110 $\tau(CH_2Cl)$

[a]The symbols correspond to the coordinates listed in Table 5. Coordinates with similar characters were added to clarify. The VCD intensities are presented as the rotational strengths, *R*, in 10^{-44} esu^2 cm^2.

As mentioned above, the modes below 1100 cm^{-1} (especially in the range 1100−900 cm^{-1}) are markedly collective, thus they must be described through the use of several internal coordinates, even in small molecules such as epichlorohydrin. Three spectral regions can be identified on the basis of the normal mode description: the methylene twisting and rocking region between 1100 and 850 cm^{-1}, the C−C and C−Cl stretching region between 850 and 700 cm^{-1}, and the C−C−C and C−C−Cl bending region between 400 and 200 cm^{-1}. A common characteristic of these modes in the three conformers is that they are all *eda* vibrations, and, as a consequence, the infrared spectra contain several intense absorptions in this region (see Figure 3). The only case of *mda* vibration in the three conformers was computed at 873, 903, and 893 cm^{-1} for I, II, and III, respectively. The main contribution to these normal modes is r(CH_2Cl), although never higher than 50% and strongly coupled with the C−C stretching vibrations, for C_{II} and C_{III}, and with the methylene twisting and rocking vibrations in the case of C_I. This different assignment has a consequence in the chiroptical activity: the VCD features are always positive, but are appreciably less intense for C_I than for the other two conformers.

A remarkable case is given by the ν(C−Cl) stretching vibration. It appears between 670 and 700 cm^{-1} in the three conformers, being largely coupled only with the bending mode of the C−C−Cl angle, labeled as ϕ(CC). The quantitative description of this normal mode is similar for the three conformers, particularly for I and II. In addition, the transition dipole moments bear also similar magnitudes, being in the three cases strongly *eda* modes. However, the VCD features are completely different, going from +28.75 au (absorbance units) for C_{III} (the highest VCD intensity of this conformer), to −9.47 au for C_{II}, and to 0.60 au for C_I. As can be observed in Figure 5, this result comes exclusively from the change of the θ angle, which is also the origin of the aforementioned deviation obtained for the ϕ(CC) coordinate. A visual evidence of all the above is the different patterns observed in the bending region of the infrared and VCD spectra among the three conformers (Figure 3). Similar behaviors are obtained by the two lower wavenumber modes, which were predicted near 200 and 100 cm^{-1} and assigned to ϕ(CC) and $\tau(CH_2Cl)$, respectively (see Figure 5).

5. CONCLUSIONS

In this work, we have addressed the relationships between the sign of the VCD intensities and the nature of the vibrational modes. These were described from a nonredundant coordinate definition, using epichlorohydrin, a relatively small size molecule containing a three-membered ring, as a model. Our set of nonredundant coordinates was successfully tested by calculating the diagonal quadratic force constants, which were consistent with the epichlorohydrin structure and provide quite similar values for the three most stable conformers. The weighted sum of the individual VCD spectra of the three lower free energy conformers accurately fitted the experimental spectrum of (*R*)-epichlorohydrin (with due differences in statistical weights, caused by the use of dilute or concentrated solutions or even for pure liquid samples). The analysis of the transition dipole moments, ETDM and MTDM, for the three most stable conformers of epichlorohydrin allowed us to understand that *mda* vibrations can be mostly found in the carbon−hydrogen vibrations. For these, stretching modes and modes of antisymmetric character have a greater magnetic nature than bending and symmetric ones, respectively. Furthermore, our data indicate that the closer is the chlorine atom to the moiety involved in the relevant normal modes, the lower the *mda* character of that normal mode. We have also observed that, within the modes with large chlorine vibrational amplitude, the angle θ between the two transition dipole moments controls widely the VCD activity. Finally, we would like to point out that nuclear displacements expressed in Cartesian coordinates usually provide us the first approach to visualize the atomic motions. However, they could be transferred to other related organic molecules or, *in primis*, to other conformers of the molecule under study, using carefully chosen roto-translation operations,[32] but not in an intuitive manner. Besides, to establish if we can give the same name to a

DOI: 10.1021/acs.jctc.5b00106
J. Chem. Theory Comput. 2015, 11, 2633−2641

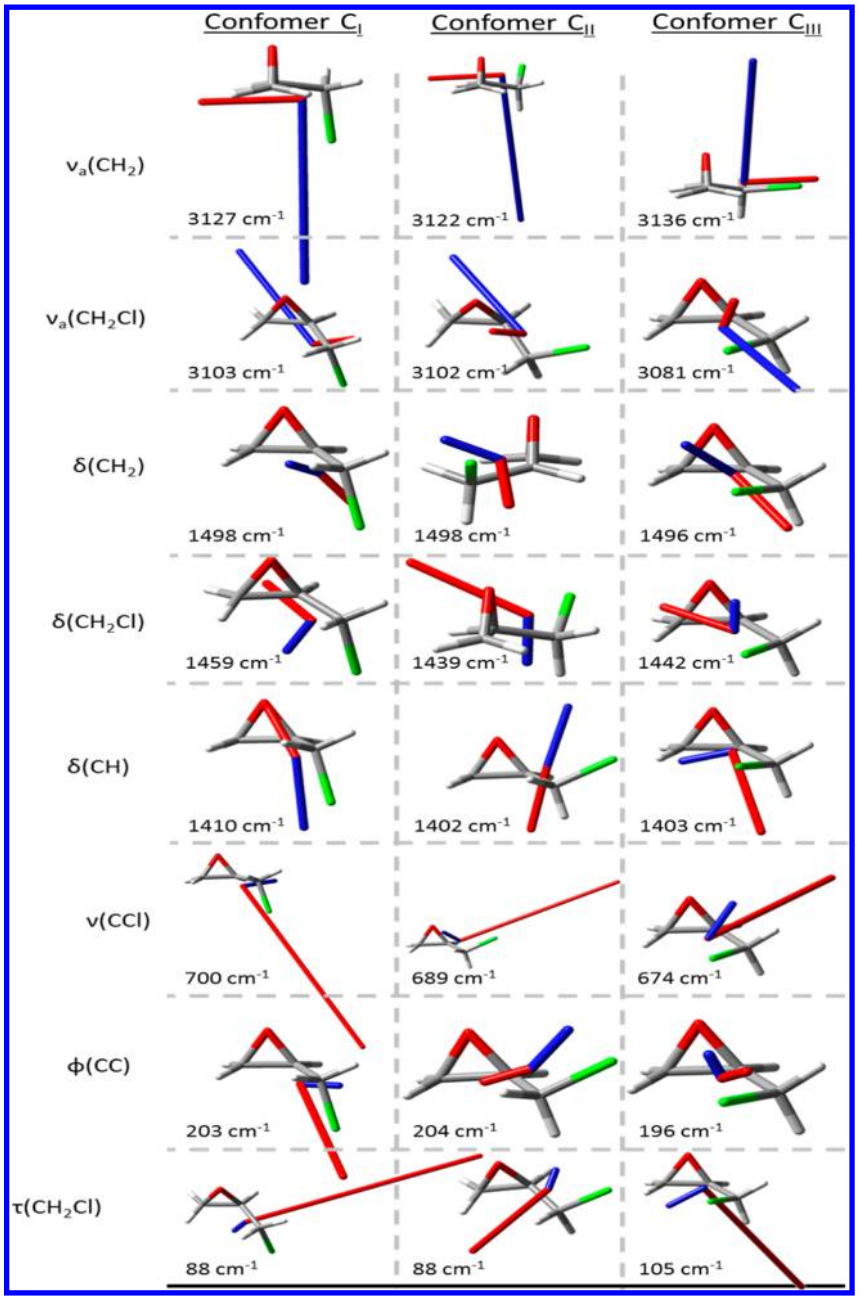

Figure 5. EDTM (red) and MDTM (blue) associated vectors to the computed wavenumbers for selected normal modes commented in the text, for each one of the three conformers of (*R*)-epichlorohydrin.

vibrational transition in two different conformers, we would need to calculate the dot product of the corresponding normal modes in terms of symmetry coordinates, which would not be possible in an immediate way for Cartesian coordinates. Only with a nonredundant set of internal coordinates we are in a firm position to address a full picture of the molecular vibrations and their relationships with the VCD intensities.

■ ASSOCIATED CONTENT

Supporting Information

The energy profile of the scanning over rotation of the side chain (Figure FS1), the experimental VCD spectra of (*R*)- and (*S*)-enantiomers of epichlorohydrin (Figure FS2) and the diagonal quadratic force constants of the three conformers of (*R*)-epichlorohydrin (Table TS1). The Supporting Information is available free of charge on the ACS Publications website at DOI: 10.1021/acs.jctc.5b00106.

■ AUTHOR INFORMATION

Corresponding Author

*E-mail: ramirez@uma.es.

Notes

The authors declare no competing financial interest.

■ ACKNOWLEDGMENTS

This work was supported by the *Ministerio de Educación, Cultura y Deporte* (Project CTQ2012-33733) and *Junta de Andalucía* (Project P09-FQM-4708). B.N.-O. is indebted to University of Málaga, *Programa de Fortalecimiento de las Capacidades en I+D+i* (FEDER).

DOI: 10.1021/acs.jctc.5b00106
J. Chem. Theory Comput. 2015, 11, 2633−2641

REFERENCES

(1) *Lord Kelvin: An Account Of His Scientific Life And Work*; Gray, A., Eds.; Kessinger Publishing, LLC: Whitefish, MT, 2007.

(2) Van't Hoff, J. H. Die Lagerung der Atome im Raume. *Arch. Neurol. Sci. Exact. Nat.* **1874**, *9*, 445−454.

(3) Ashvar, C. S.; Devlin, F. J.; Stephens, P. J. Molecular Structure in Solution: An ab Initio Vibrational Spectroscopy Study of Phenyloxirane. *J. Am. Chem. Soc.* **1999**, *121*, 2836−2849.

(4) Gigante, D. M. P.; Long, F.; Bodack, L. A.; Evans, J. M.; Kallmerten, J.; Nafie, L. A.; Freedman, T. B. Hydrogen stretching vibrational circular dichroism in methyl lactate and related molecules. *J. Phys. Chem. A* **1999**, *103*, 1523−1537.

(5) Tam, C. N.; Bour, P.; Keiderling, T. A. Vibrational Optical Activity of (3S,6S)-3,6-Dimethyl-1,4-dioxane-2,5-dione. *J. Am. Chem. Soc.* **1996**, *118*, 10285−10293.

(6) *Introduction to Modern Vibrational Spectroscopy*; Diem, M., Ed.; Wiley: New York, 1993; pp 240−260.

(7) McCann, J. L.; Rauk, A.; Wieser, H. A conformational study of (1S,2R,5S)-(+)-menthol using vibrational circular dichroism spectroscopy. *Can. J. Chem.* **1998**, *76*, 274−283.

(8) Polavarapu, P. L.; Zhao, C.; Cholli, A.; Vernice, G. Vibrational Circular Dichroism, Absolute Configuration, and Predominant Conformations of Volatile Anesthetics: Desflurane. *J. Phys. Chem. B* **1999**, *103*, 6127−6132.

(9) *Vibrational Optical Activity: Principles and Applications*; Nafie, L. A., Ed.; Wiley: Chichester, 2011; pp 1−30.

(10) Setnička, V.; Urbanová, M.; Bouř, P.; Král, V.; Volka, K. Vibrational Circular Dichroism of 1,1'-Binaphthyl Derivatives: Experimental and Theoretical Study. *J. Phys. Chem. A* **2001**, *105*, 8931−8938.

(11) Kawamura, K.; Ohta, T.; Otani, G. An Efficient Synthesis of the Optical Isomers of Nipradilol. *Chem. Pharm. Bull.* **1990**, *38*, 2092−2096.

(12) Wang, F.; Polavarapu, P. L. Conformational Stability of (+)-Epichlorohydrin. *J. Phys. Chem. A* **2000**, *104*, 6189−6196.

(13) Stephens, P. J.; Devlin, F. J.; Chabalowski, C. F.; Frisch, M. J. Ab Initio Calculation of Vibrational Absorption and Circular Dichroism Spectra Using Density Functional Force Fields. *J. Phys. Chem.* **1994**, *98*, 11623−11627.

(14) Becke, A. D. Density-functional thermochemistry. III. The role of exact exchange. *J. Chem. Phys.* **1993**, *98*, 5648−5652.

(15) Kim, K.; Jordan, K. D. Comparison of Density Functional and MP2 Calculations on the Water Monomer and Dimer. *J. Phys. Chem.* **1994**, *98*, 10089−10094.

(16) Yanai, T.; Tew, D. P.; Nicholas, N. C. A new hybrid exchange−correlation functional using the Coulomb-attenuating method (CAM-B3LYP). *Chem. Phys. Lett.* **2004**, *393*, 51−57.

(17) Hariharan, P. C.; Pople, J. A. The Influence of Polarization Functions on Molecular Orbital Hydrogenation Energies. *Theor. Chim. Acta* **1973**, *28*, 213−222.

(18) Clark, T.; Chandrasekhar, J.; Spitznagel, G. W.; Schleyer, P. V. R. Efficient diffuse function-augmented basis sets for anion calculations. III. The 3-21+G basis set for first-row elements, Li−F. *J. Comput. Chem.* **1983**, *4*, 294−301.

(19) Miertus, S.; Scrocco, E.; Tomasi, J. Electrostatic interaction of a solute with a continuum. A direct utilizaion of ab initio molecular potentials for the prevision of solvent effects. *J. Chem. Phys.* **1981**, *55*, 117−129.

(20) Miertus, S.; Tomasi, J. Approximate evaluations of the electrostatic free energy and internal energy changes in solution processes. *Chem. Phys.* **1982**, *65*, 239−245.

(21) *Molecular Vibrations: The Theory of Infrared and Raman Vibrational Spectra*; Wilson, E. B., Decius, J. C., Cross, P. C., Eds.; McGraw-Hill: New York, 1955; pp 54−74.

(22) *Vibrational States*; Califano, S., Ed.; Wiley: London, 1976; pp 120−145.

(23) *Theory and Methods of Calculations of Molecular Spectra*; Gribov, L. A., Orville-Thomas, W. J., Eds.; Wiley: New York, 1988; pp 150−170.

(24) *Vibrational Intensities in Infrared and Raman Spectroscopy*; Zerbi, G., Ed.; Elsevier: Amsterdam, 1984; pp 70−90.

(25) Pulay, P.; Fogarasi, G.; Pongor, G.; Boggs, J. E. Systematic ab initio gradient calculation of molecular geometries, force constants, and dipole moment derivatives. *J. Am. Chem. Soc.* **1979**, *101*, 2550−2560.

(26) Fogarasi, G.; Zhou, X.; Taylor, P. W.; Pulay, P. The calculation of ab initio molecular geometries: efficient optimization by natural internal coordinates and empirical correction by offset forces. *J. Am. Chem. Soc.* **1992**, *114*, 8191−8201.

(27) Gussoni, M.; Dellepiane, G.; Abbate, S. The inverse of a rectangular matrix: Some applications in molecular dynamics. *J. Mol. Spectrosc.* **1975**, *57*, 323−330.

(28) Longhi, G.; Ricard, L.; Abbate, S.; Zerbi, G. Electric dipole moment functions from vibrational absorption intensities of fundamental and overtone transitions. *J. Chem. Phys.* **1988**, *88*, 6733−6742.

(29) *Linear Dichroism and Circular Dichroism*; Nordén, B., Rodger, A., Dafforn, T., Eds.; RSC: London, 2010; pp 184−208.

(30) Nicu, V. P.; Baerends, E. J. Robust normal modes in vibrational circular dichroism spectra. *Phys. Chem. Chem. Phys.* **2009**, *11*, 6107−6118.

(31) Abbate, S.; Longhi, G.; Castiglioni, E. Near-infrared vibrational circular dichroism: NIR-VCD. In *Comprenhensive Chiroptical Spectroscopy*, 1st ed.; Berova, N., Polavarapu, P. L., Nakanishi, K., Woody, R., Eds.; John Wiley & Sons Ltd.: Hoboken, NJ, 2012; Vol. *1*, pp 247−274.

(32) Bour, P.; Sopkova, J.; Bednarova, L.; Malon, P.; Keiderling, T.A. *J. Comput. Chem.* **1997**, *18*, 664−659.

DOI: 10.1021/acs.jctc.5b00106
J. Chem. Theory Comput. 2015, 11, 2633−2641